RESEARCH PAPER

Scale-up and control of droplet production in coupled microfluidic flow-focusing geometries

Molly K. Mulligan · Jonathan P. Rothstein

Abstract A single microfluidic chip consisting of six microfluidic flow-focusing devices operating in parallel was developed to investigate the feasibility of scaling microfluidic droplet generation up to production rates of hundreds of milliliters per hour. The design utilizes a single inlet channel for both the dispersed aqueous phase and the continuous oil phase from which the fluids were distributed to all six flow-focusing devices. The exit tubing for each of the six flow-focusing devices is separate and individually plumbed to each device. Within each flow-focusing device, the droplet size was monodisperse, but some droplet size variations were observed across devices. We show that by modifying the flow resistance in the outlet channel of an individual flow-focusing device it is possible to control both the droplet size and frequency of droplet production. This can be achieved through the use of valves or, as is done in this study, by changing the length of the exit tubing plumbed to the outlet of the each device. Longer exit tubing and larger flow resistance is found to lead to larger droplets and higher production frequencies. The devices can thus be individually tuned to create a monodisperse emulsion or an emulsion with a specific drop size distribution.

Keywords Droplet production · Microfluidics · Scale-up · Flow focusing

M. K. Mulligan · J. P. Rothstein (✉)
Department of Mechanical and Industrial Engineering,
University of Massachusetts, 160 Governors Drive, Amherst,
MA 01003, USA
e-mail: rothstein@ecs.umass.edu

1 Introduction

Droplet generation in microfluidic devices is a well-understood and studied phenomena, which is attracting increasing attention owing to a variety of potential applications in biology, medicine, chemistry and a wide range of industries (Shu et al. 2007; Dollet et al. 2008; Li et al. 2008). Microfluidic devices are capable of producing monodisperse droplets through a number of different methods including colliding jets, T-junctions, cross-flowing, co-flowing and flow-focusing devices (Christopher and Anna 2007). Microfluidic drop generation thus lends itself to a variety of industrial emulsification applications where precisely controlled monodisperse, bidisperse or even precisely polydisperse emulsion droplets are desirable (Anna et al. 2003; Miller et al. 2010). The challenge is one of scale. A single microfluidic droplet creation device can produce droplets at a rate of tens to hundreds of microliters per minute. Unfortunately, this production rate is several orders of magnitude below the throughput needed for most industrial applications (Barbier et al. 2006). Several recent papers have investigated the possibility of scaling up microfluidic devices by placing a number of droplet generators in parallel (Li et al. 2008; Barbier et al. 2006; Garstecki et al. 2008; Nisisako and Torii 2008; van Dijke et al. 2009; Kobayashi et al. 2010).

The most successful scale-up of microfluidic droplet production was derived from the field of membrane emulsification (Vladisavljevic and Williams 2005) where the disperse phase is driven through a porous membrane into a reservoir of the continuous phase. Droplets are formed at the exit of the pore and often convected away using a cross flow or stirring motion to avoid coalescence (Vladisavljevic and Williams 2005). These techniques have been refined over the last few years by a number of groups

that have used micromachining of stainless steel (Kobayashi et al. 2008) and silicon-based lithography techniques (van Dijke et al. 2009; Kobayashi et al. 2010; Vladisavljevic et al. 2011) to produce membranes with precise arrays of slots and through holes. The diameter of the droplets produced is directly related to the size of the holes or slots from which they are produced. As a result, droplets from 1 μm to several mm can easily be produced with these techniques with the coefficient of variation of the drop diameter typically between 3 and 15% (van Dijke et al. 2009; Kobayashi et al. 2002, 2008, 2010; Vladisavljevic and Williams 2005; Vladisavljevic et al. 2011). Although these techniques are relatively easy to scale-up, shear-based microfluidic techniques such as flow-focusing and T-junctions have been shown to result in more monodisperse droplets and a larger production rate of droplets per device (Christopher and Anna 2007; van Dijke et al. 2009). Thus, it is important to develop designs that easily and efficiently parallelize shear-based devices.

The ideal design for a highly parallelized shear-based microfluidic drop generating device is still an active area of research primarily because of the interplay that can occur between a number of devices operating in parallel (Li et al. 2008; Barbier et al. 2006; Garstecki et al. 2008; Nisisako and Torii 2008; Kumacheva et al. 2009). Using the T-junction method of droplet formation, Barbier et al. (2006) studied the behaviors of two droplet production devices operating in parallel. The dynamics of droplet formation in this device were described as complex, owing to the fact that there were several different modes of droplet formation including synchronization, quasi-periodic and chaotic droplet production. Droplet production frequency was found to increase with the increase in the water, dispersed, phase flow rate, as is typical for T-junction droplet creation devices. In the synchronized droplet creation regime monodisperse droplets were produced. This type of droplet creation was achieved but having the legs of the two T-junctions be identical in length. For the quasi-periodic droplet formation mode, when both legs of the T-junction are the same length, the droplets have a polydispersity in the order of 8% in each leg of the device. In the chaotic regime, droplet polydispersity ranged from 30 to 60%. When the T-junction legs were of different length the polydispersity of droplet production was large and droplet production was chaotic and not synchronized (Barbier et al. 2006).

Garsetcki et al. (2008) looked at the process of scaling up microfluidic flow-focusing droplet creation devices. Using a common inlet for the continuous phase solution, a common outlet for the droplets produced and individual inlets for the dispersed phase fluid, Garstecki et al. (2008) sought to understand the coupling dynamics of droplet and bubble generation in parallel microfluidic flow-focusing

droplet production. It was found that the mechanism of interaction between the coupled droplet generators depended on the compressibility of the dispersed phase fluid. Parallel bubble formation, using gas as the dispersed phase, was found to have complicated formation dynamics due to the compressibility of the gas dispersed phase. Droplet formation was not found to be coupled over the range of flow rates studied (Garstecki et al. 2008).

More recently, Nisisako and Torii (2008) designed a highly parallelized drop generating device consisting of 128 co-flowing cross-junctions arranged in a radial pattern around a common outlet to produce single and double emulsions. A three-dimensional support structure was fabricated so that a single inlet and pump could be used to deliver the continuous and disperse phase. In their most highly parallelized device, 320 ml/h of a monodisperse oil in water emulsion was successfully produced. The resulting droplet diameter was 96 μm with a coefficient of variation of 1.3%. Janus droplets of similar diameters and polydispersities were also produced at a slightly low rate (Nisisako and Torii 2008). The production rate of droplets in this shear-based cross-junction device is significantly larger than microfluidic membrane emulsification devices which typically produce much less than 100 ml/h of emulsion (Nisisako and Torii 2008; Vladisavljevic et al. 2011). In the flow regime where monodisperse droplets were produced, the formation of droplets in neighboring cross-junctions was coupled with droplet formation and break-up alternating from one to the other.

An interesting application of microfluidic droplet creation devices is using these devices to create monodisperse microparticles (Xu et al. 2005). A recent study focused on using parallel droplet generation using a flow-focusing droplet creation geometry to create polymer microparticles in parallel (Kumacheva et al. 2009). Common inlets were used for the continuous phase and dispersed phase that fed into each of the parallel droplet generators, and a common outlet was used for the particles produced in the parallel droplet creator. This work found that microfluidic devices could be used to produce polymer microparticles at a rate of 50 g/h with a maximum polydispersity of 5%. In this work, where all devices were fed through common inlets and outlets, hydrodynamic coupling between the parallel microfluidic droplet generators was observed. The pressure variations caused by droplet formation in a single droplet generator affected the adjacent droplet generators and caused a broadening of the size distribution of droplets generated. It was also found that by varying the length of the dispersed phase inlet polydispersity of droplet size could be controlled, but this also depended upon flow rate ratio (Kumacheva et al. 2009).

Li et al. (2008) looked at the coupling between four parallel flow-focusing droplet generators with all the same

dimensions and then with four different droplet generators which had differently sized orifices for droplet generation. While, the droplets could be considered monodisperse by NIST Size Standards (Li et al. 2008), the broadening in the size distribution of droplets produced in the four identical droplet generators was attributed to the coupling between the droplet generators due to droplet formation in an adjacent droplet generator. For parallel droplet generation when the four droplet generators had different orifice dimensions monodisperse droplets were produced over the entire range of flow rates for the two droplet generators with the widest orifices. For the droplet generators with the two narrowest orifices, at low flow rates each generator created droplets of different sizes each with a small polydispersity. For flow rate ratios between 8 and 10, all four droplet generators produced the same size monodisperse droplets (Li et al. 2008).

For a highly parallelized microfluidic device to be successfully implemented in industry, it should be designed in such a way that it can achieve the desired production rates while, like the device of Nisisako and Torii (2008), minimizing the amount of plumbing and, more importantly, pumping required. Ideally, a parallel microfluidic droplet creation device would have just a single input for both the dispersed and continuous phases of the emulsion so that both phases could be driven with a single pump from a single, common source of fluid. For a two-dimensional microfluidic device fabricated entirely from PDMS, having a common inlet for both the dispersed and continuous phases necessitates individual outlets for each of the flow-focusing devices. In this paper, we will show that this design has a number of key advantages. First, having separate outlets reduces coupling between flow-focusing devices and avoids some of the complex dynamics that result. Second, this device design allows one to modify the flow resistance in the outlet of each of the flow-focusing devices individually either by adding a valve or, in the case of this work, by varying the length of the outlet tubing plumbed into each droplet generator. We will show that changing the flow resistance in the outlet tubing can have a large impact on both droplet size and frequency making it possible to generate a truly monodisperse emulsion across a number of flow-focusing devices in parallel or to create an emulsion with a specifically designed droplet size distribution.

2 Experimental

The microfluidic flow cell used in these experiments is shown schematically in Fig. 1a. The flow cell was designed to have six parallel flow-focusing droplet generators with identical dimensions. The number of parallel flow-focusing

devices was limited by the area of the silicon wafers used, but in general, the number of parallel devices could be expanded if a larger wafer or a more condensed design were used. In Fig. 1b, a close-up is shown of one of the individual flow-focusing geometries with relevant dimensions labeled. Parallel microfluidic droplet generators were fabricated in PDMS using standard soft lithography methods and a PDMS ratio mismatch for sealing (Miller et al. 2010; Anderson et al. 2000; McDonald et al. 2000; McDonald and Whitesides 2002; Mulligan and Rothstein 2011). The masks used for the fabrication of master wafers were printed on a high-resolution transparency with a resolution of 20,000 dpi, thus allowing for features as small as 10 μm. The depth of the devices was 250 μm.

All experiments were carried out on an inverted microscope (Nikon TE2000-U) and video data was recorded using a high-speed CCD video camera (Vision Research, Phantom 4.6). The continuous phase fluid for all experiments was light mineral oil, which has a viscosity of $\mu_c = 47$ mPa s (Fisher Scientific Brand). The dispersed phase was a surfactant solution containing 5 mM cetylpyridinium chloride (CPyCL) in distilled/deionized water. Flow through the microfluidic device was driven by two stepper-motor actuated micro-syringe pumps (New Era Pump Systems, NE-500 OEM). The flow of the dispersed phase, Q_d, was held constant throughout the experiments at
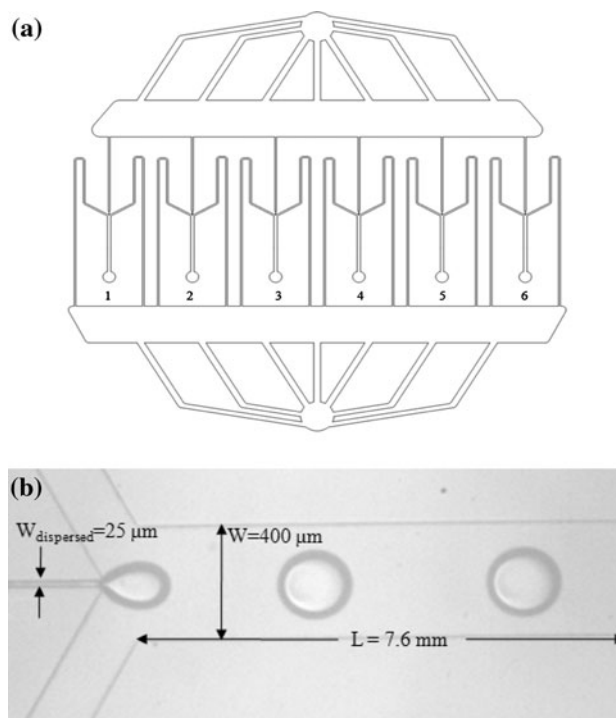
Fig. 1 a Schematic of the six parallel flow-focusing device geometry with a common inlet for the dispersed and continuous phase fluids and individually plumbed outlets. **b** Image of a single flow-focusing device with the relevant dimensions labeled

$Q_d = 20$ μL and the continuous phase flow rate, Q_c, was varied to investigate the effect of flow rate ratio, $Q_r = Q_c/Q_d$, on droplet production.

3 Results and discussion

Using the microfluidic device described in the previous section, droplets were produced in the six parallel flow-focusing geometries simultaneously and the effect of flow rate ratio and exit tubing lengths on droplet size and frequency was studied. In Fig. 2, a series of representative images are presented showing droplet generation in each of the flow-focusing geometries within the parallel droplet generation device. Here the flow rate ratio is set to $Q_r = 5$ and the outlet tubing is set to 20 cm for each channel. Note that the images in Fig. 2 are not correlated in time because the microscope had to be translated to capture the droplet formation in each channel. The images show that within any individual channel, the resulting droplet size is monodisperse. Small standard deviations of less than one pixel were measured. At these magnifications, this corresponds to less than a 3 μm standard deviation for droplets as big as 180 μm in radius or a coefficient of variation of about 2%.

In Fig. 2, a clear variation in frequency of droplet production can be observed with channels 2, 5 and 6 producing droplets at a significantly larger rate than the rest. These variations across the device are likely due to the specific design of the inlet manifolds used to supply the oil and aqueous phases to the flow-focusing geometries. The frequency of droplet production is quantified in Fig. 3 for each of the six channels across a wide range of flow rate ratios. At the lowest flow rate ratio, droplet production frequencies in each channel are all around the same frequency with a standard deviation of 1.2 Hz for $Q_r = 1$. As the flow rate ratio increases, both the frequency of droplet production and its standard deviation were found to increase. In Fig. 2, a slight variation in droplet size produced across the six flow-focusing geometries can be observed, although it is less obvious than the variation in droplet frequency.

For scale-up to be successful, the variation of droplet size across all the parallel flow-focusing geometries should be small enough that the resulting emulsion can be considered monodisperse. Shown in Fig. 4 is a plot of measurements of the droplet radius as a function of the flow rate ratio for all six channels in a single device with the exit tubing set to an equal length of 10 cm for each channel. When all six of the droplet creation devices are taken into account, the range of droplet sizes has a larger variation than that found for a single flow-focusing droplet creation device which is shown in Fig. 4 by the representative error
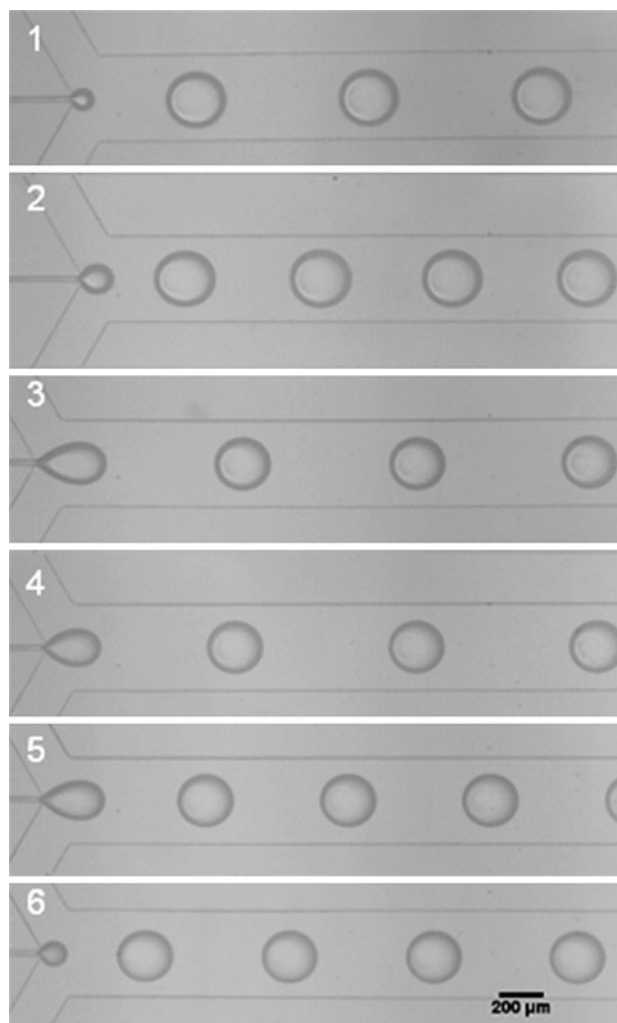
Fig. 2 Representative composite image of the droplets in each of the six flow-focusing devices within the parallel droplet generation device. All the exit tubes have an equal length of 20 cm and the global flow rate ratio is $Q_r = 5$

bars on the data from channel 2. At a flow rate ratio of $Q_r = 1$, the radii of the droplets varied between $155 \leq r \leq 179$ μm. The average droplet radius was $r = 172$ μm with a standard deviation of 9 μm. The 5% coefficient of variation for the droplets could be the result of either the design of the parallel droplet generating device or differences in channel height or width introduced during the fabrication of the wafer or both. A close inspection of the droplet radii across the device reveals that the two outermost flow-focusing devices, device numbers one and six, are the clear outliers in the data. This suggests that the edge effects of the inlet manifolds used to supply the oil and water phases to each of the flow-focusing geometries are having a significant effect on the droplet sizes generated in the outermost devices. This can be an issue if one is to implement such a scale-up scheme to achieve monodisperse droplet distribution, but it could be
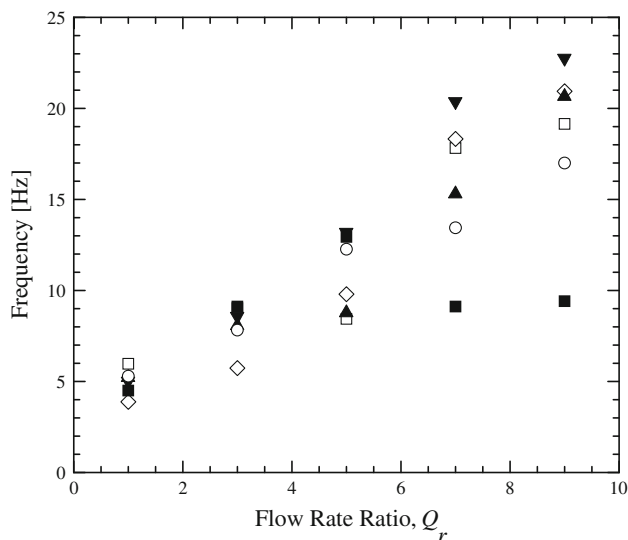
Fig. 3 The frequency of droplet production in each channel when all of the channels have equal length exit tubing of 20 cm. The symbols for each channel are as follows: one (*open square*), two (*inverted filled triangle*), three (*open diamond*), four (*filled triangle*), five (*open circle*) and six (*filled square*)

Fig. 4 Droplet radius as a function of flow rate ratio for all six microfluidic flow-focusing devices on the chip with exit tubing length equal to 20 cm for all channels. The symbols for each channel are as follows: one (*open square*), two (*inverted filled triangle*), three (*open diamond*), four (*filled triangle*), five (*open circle*) and six (*filled square*)

largely mitigated by a redesign of the inlet reservoirs and the channels feeding them. If one removes the outer two channels, the standard deviation of droplet size across all channels at each flow rate decreases significantly. For a flow rate ratio of $Q_r = 1$, the droplet radius across channels two through five varies between $170 \leq r \leq 179$ μm with a standard deviation of 3.8 μm or a coefficient of variation of about 2%. With individually plumbed outlets, one can obtain a more monodisperse emulsion by removing these small droplets from the product stream. However, it is desirable to develop a technique that would allow modifying the droplet size produced within each individual flow-focusing geometry without having to redesign the microfluidic device or throw away one-third of the emulsion.

The objective is thus to tune the flow cell such that all channels are producing monodisperse droplets, meaning that the radii of the droplets have less than 5% variation across all six channels, not just the inner four channels. As seen in Fig. 4, the radius of the droplets produced within a single flow-focusing geometry are a strong function of flow rate ratio. A factor of two change in the droplet diameter can be achieved by a tenfold change in the flow rate ratio. Additionally, if the flow rate ratio is held fixed, the droplet size has been shown to decrease with increasing total flow rate (Miller et al. 2010). If the flow resistance within the outlet of one of the flow-focusing geometries is increased either through the addition of a valve or through an increase in the length of exit tubing, one would expect an increase in the resulting drop size due to the reduction in

the total flow rate through that outlet tubing. However, due to the multiple phases and the multiple flow-focusing geometries in parallel, the results are slightly more complicated.

For a single-phase fluid, the pressure drop in the microfluidic channel downstream of the flow-focusing geometry is given by (White 1991)

$$\Delta p = -\frac{Q\mu l}{8ba^3} \left(1 - \frac{192a}{\pi^5 b} \sum_{i=1,3,5}^{\infty} \frac{Tanh(i\pi b/2a)}{i^5} \right)^{-1} \quad (1)$$

where Q is the total volume flow rate input into the system, μ is the viscosity, l is the length of the channel, b is half the height of the channel, a is half the width of the channel and p is the pressure. This pressure drop is the same for all six channels independent of the outlet tubing length. For the circular outlet tubing with an inner radius of $r = 0.0265$ mm, the pressure drop becomes (White 1991)

$$\Delta p = -\frac{4Q\mu l}{3\pi r^4}. \quad (2)$$

For a 10-cm long outlet tubing, the pressure drop due to the microfluidic channel is approximately equal to that of the exit tubing. Increasing the exit tubing length from 10 cm to 1 m increases the pressure drop in the outlet tubing by a factor of ten and the total pressure drop from the flow-focusing geometry by a factor of more than five. More precisely, we should discuss a fivefold increase in flow resistance and reduction in volume flow rate because all six flow-focusing geometries are operating between two

common reservoirs and the total pressure drop in each should be the same.

In order to minimize the number of complexities of the experiments, the outlet tubing lengths of all the flow-focusing geometries except for channel four will be held fixed at 10 cm. The length of the outlet tubing in channel four will be varied from 10 cm to 1 m to investigate the impact that a fivefold increase in flow resistance can have on the droplet size and frequency at various flow rate ratios. In Fig. 5, a series of representative images are presented showing droplet generation in each of the flow-focusing geometries within the parallel droplet generation device. Here the flow rate ratio is again set to $Q_r = 5$ as it was in Fig. 2, but now all the outlet tubing is set to 10 cm except for channel 4 which has an exit tubing length of 50 cm. The results are quite striking. The size of drops produced in flow-focusing geometry number 4 is significantly larger than the drops in the other channels. In addition, the frequency of drop production in channel 4 has increased substantially. The droplet size in the other channels has not changed significantly from the base case where all of the outlet tubing was 20 cm long, however, the frequency of droplet production has been reduced considerably.

In Figs. 6 and 7, the drop size and frequency of channel 4 is compared to the average drop size and frequency produced from the base case where all the flow-focusing geometries had 20-cm-long outlet tubing. The largest increases in drop size, both as an absolute and as a percentage of the base drop size, were observed at the lowest flow rate ratios. In some cases, an increase in drop size of nearly 20% was observed. The effectiveness of increasing the outlet flow resistance is found to decay with increasing flow rate ratio. This is in large part due to the reduction in sensitivity of drop size on changes to flow rate ratio as seen in Fig. 6 as the flow rate ratio increases. Note, however, that at a flow rate ratio of $Q_r = 9$, the average diameter of the drop produced from channel 4 are slightly smaller than those produced from the channels with the shorter exit tubing. We will come back to this observation later when we discuss the effect of variations in exit tubing length.

The overall flow rates of each phase are set by the syringe pumps. However, the flow rate of water and oil within each of the six flow-focusing geometries is not fixed, but can vary locally. As seen in Fig. 7, for the case of the 50-cm-long outlet tubing, the frequency of droplet production was found to increase above the base case for all of the flow rate ratios studied. The frequency of droplet production can be combined with the droplet radius to calculate the total volume flow rate of water through channel 4. The resulting volume flow rate of water was found to be between two and four times larger than the base case when all outlet tubing was set to 20 cm. The biggest
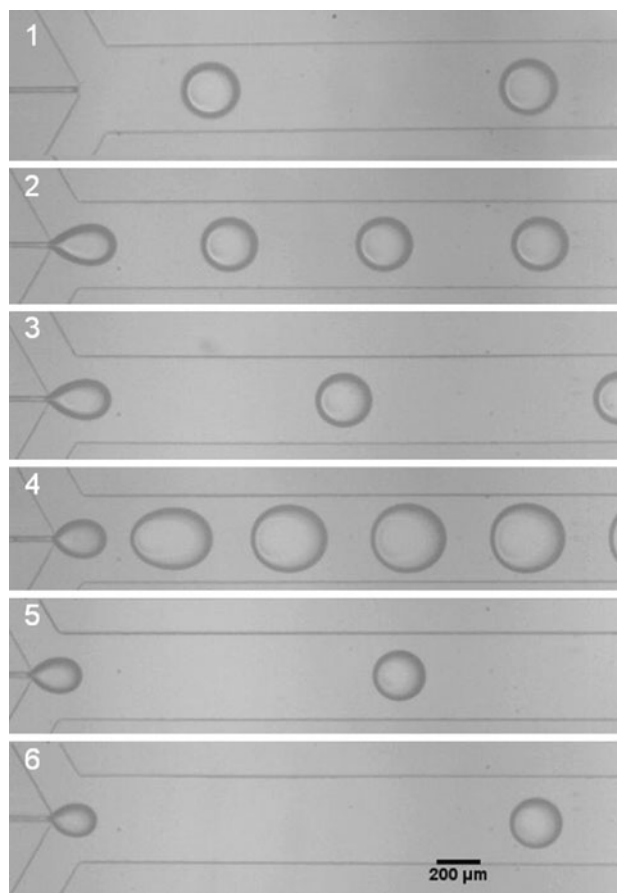
Fig. 5 Representative composite image of the droplets in each of the six flow-focusing devices within the parallel droplet generation device. All of the outlet tubes are 10 cm long except channel 4 which is 50 cm long. The flow rate ratio is globally set to $Q_r = 5$
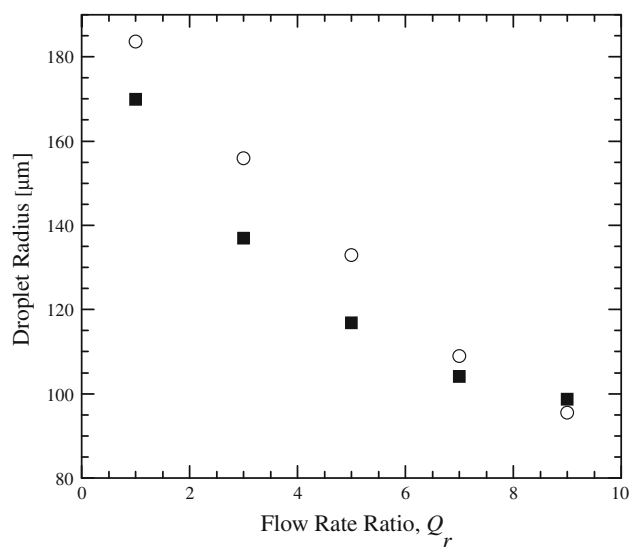
Fig. 6 Droplet radius as a function of flow rate ratio comparing channels with 10-cm-long outlet tubing (*filled square*) to channel 4 (*open circle*) which had exit tubing 50 cm long
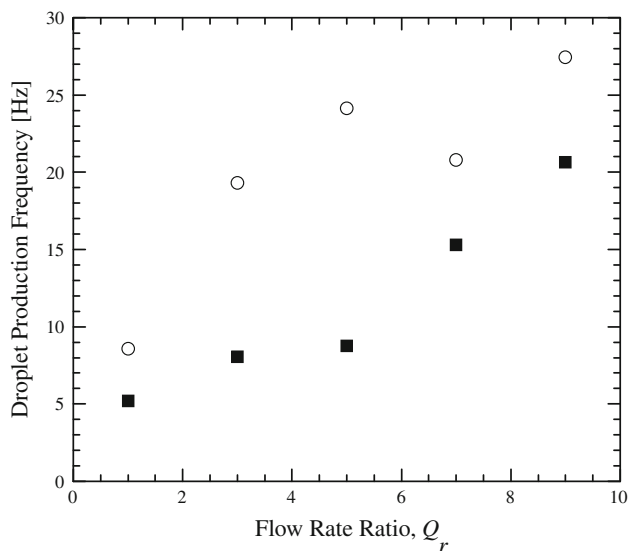
Fig. 7 Droplet production frequency as a function of flow rate ratio comparing channels with 10-cm-long outlet tubing (*filled square*) to channel 4 (*open circle*) which had exit tubing 50 cm long

differences were observed for flow rate ratios of $Q_r = 3$ and 5, where the largest changes to droplet size was also found.

With a longer outlet tube, the flow rate of the continuous oil phase within the flow-focusing geometry is significantly reduced. In the absence of tip streaming, it has been shown that due to the reduction of shear stress acting on the dispersed phase as droplets are produced within a flow-focusing geometry, that at a fixed flow rate ratio, Q_r, the average droplet radius increases with an decrease in the total flow rate, $Q_{Total} = Q_c + Q_d$ (Miller et al. 2010). In the experiments presented in Figs. 5, 6, 7, the flow rate ratio in channel 4 is not fixed to the global value, Q_r, set at the syringe pumps, but is found to be significantly lower than in the other five channels. As a result, the droplet size presented in Fig. 6 are even larger than one would predict if the flow rate ratio were held fixed. The increased water flow rate observed in channel 4 is due in large part to the difference in viscosity between the dispersed and continuous phases. The viscosity of the dispersed phase is $\mu_{water} = 1$ mPa s and the viscosity of the continuous phase is $\mu_{oil} = 47$ mPa s. At the center of the channel, the shear rate is zero and increases linearly towards the walls. As a result, a small water drop convecting along the center of the channel contributes very little to the overall pressure drop in the channel. As a water droplet increases in size, it begins to experience the higher shear rates near the channel wall. Thus, for the same total volume flow rate, q_{total}, the pressure drop in the channel is reduced due to the contribution of the low viscosity water phase. As a result, the total pressure drop across this parallel microfluidic device

is minimized by increasing the volume flow rate of water in the flow-focusing geometry, channel 4, where the outlet tubing length and therefore the flow resistance was largest.

The drop size within a given channel can be tuned by varying the flow resistance. In Fig. 8, the droplet size in channel 4 is presented as a function of flow rate ratio for exit tubing lengths varying from 10 cm to 1 m. As the length of tubing was increased from 10 to 25 cm and finally to 50 cm, the flow resistance in channel 4 increased. For these lengths of tubing, with an increased flow resistance, the size of the droplets produced in channel 4 was found to increase demonstrating that downstream flow resistance could be used to effectively tune the size of droplets produced in flow-focusing geometries. It appears, however, that additional flow resistance imposed by the 50 cm of exit tubing maximizes the droplet size variation that can be induced within our microfluidic drop-generating device. For larger tubing lengths, the flow resistance and resulting pressure drop in the device is large enough to eliminate droplet production in channel 4 at high flow rate ratios. For the 75-cm-long exit tubing tested, no water droplets could be produced in channel 4 above a flow rate ratio of $Q_r > 7$, while for the 1-m-long exit tubing, droplets could not be produced above $Q_r > 1$. Additionally, as was seen to a lesser extent with the 50-cm-long exit tubing, for the 75-cm-long exit tubing, both the size and frequency of droplet production, as seen in Fig. 9, are found to reduce below the base 10 cm case. This demonstrates the complexity of designing a microfluidic device containing a number of flow-focusing device producing droplets in parallel. It also motivates the need for detailed multiphase numerical simulations (Dijke et al. 2008) to be performed in the future to better understand these complex flow phenomena.

4 Conclusions

Using a series of six flow-focusing geometries in parallel, aqueous droplets in oil were created simultaneously on a single microfluidic device. The need to create droplets in parallel droplet generators arises from the need for higher output of droplets from microfluidic devices so that these devices can be utilized in industrial settings. The design presented here has a single input for both the continuous and dispersed phases and separate exit tubes for each of the flow-focusing channels on the chip. The single inlet for the continuous and disperse phases minimizes both the plumbing and pumping requirements for this highly parallelized device. The use of individual exit tubes for each flow-focusing device reduces coupling between flow-focusing devices and avoids some of the complex dynamics that result. Additionally and most importantly,
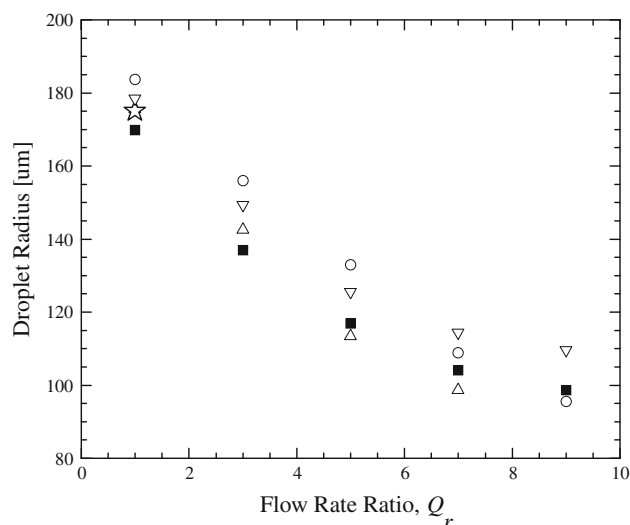
Fig. 8 Droplet radius as a function of flow rate ratio for channel four with varying outlet tubing length. The outlet tubing length was varied from 10 cm (*filled square*), which was the length of each of the other outlet tubing lengths, to 24 cm (*inverted triangle*), 50 cm (*open circle*), 75 cm (*open triangle*) and 100 cm (*star*)
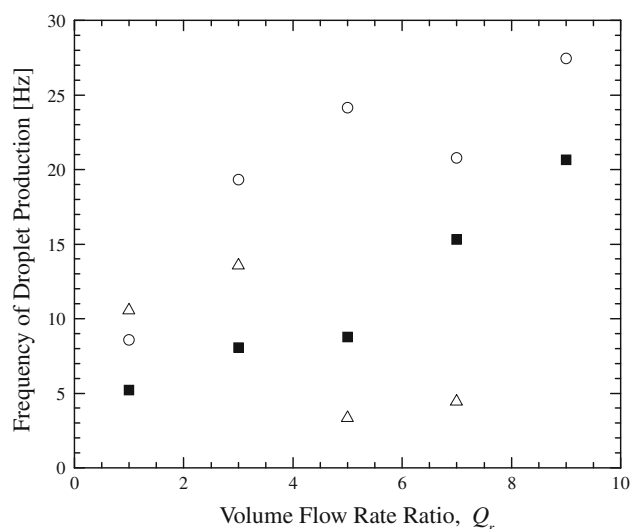
Fig. 9 Frequency of droplet production as a function of flow rate ratio for channel four with varying outlet tubing length. The outlet tubing length was varied from 10 cm (*filled square*), which was the length of each of the other outlet tubing lengths, to 50 cm (*open circle*) and 75 cm (*star*)

we show that having separate exit tubes allows the users to tune both the size and production frequency of the droplets in individual channels to generate emulsions that are either monodisperse or contain a specifically prescribed drop size distribution. This was accomplished by changing the length of the exit tubing from 10 cm to 1 m in order to increase the flow resistance in order to increase the flow resistance, although a similar result could have been achieved using valves.

When all six channels had equal length exit tubing and therefore an equal downstream flow resistance, the coefficient of variation in the droplet size was found to be roughly 5% across all six flow-focusing devices. The largest variation occurred in the outer two channels of the device where end effects in the inlet reservoirs of the continuous and disperse phase had an effect. Here, we show that it is possible to correct for the imperfections in the initial device design to achieve a monodisperse emulsion by tuning the droplet size by varying the downstream flow resistance in a given channel. With all other exit tubing lengths held fixed, the exit tubing length and therefore the flow resistance of channel 4 was increased systematically increased from 10 cm to 1 m. As the tubing length was increase from 10 to 50 cm, the droplet size and frequency of droplet production were found to increase by as much as 20% at a given global ratio of the continuous to disperse flow rates. The size of the droplets produced in the other five channels did not significantly change, but their frequency was found to decrease significantly. Beyond a downstream tubing length of 50 cm, the increased flow resistance was large enough to eliminate droplet production at the higher flow rates.

Thus, this study clearly shows that, scaling up microfluidic devices for high output droplet production is possible. Using the device design presented here, scale-up can be achieved with minimal plumbing and pumping and with a high degree of control over droplet size and production frequency.

References

Anderson JR, Chiu DT, Jackman RJ, Cherniavskaya O, McDonald JC, Wu HK, Whitesides SH, Whitesides GM (2000) Fabrication of topologically complex three-dimensional microfluidic systems in PDMS by rapid prototyping. Anal Chem 72:3158–3164

Anna SL, Bontoux N, Stone HA (2003) Formation of dispersions using 'flow focusing' in microchannels. App Phys Lett 82:364–366

Barbier V, Willaime H, Tabeling P, Jousse F (2006) Producing droplets in parallel microfluidic systems. Phys Rev E 74:046306

Christopher GF, Anna SL (2007) Microfluid methods for generating continuous droplet streams. J Phys D Appl Phys 40:R319–R336

Dijke KCv, Schroe KCPGH, Boom RM (2008) Microchannel emulsification: from computational fluid dynamics to predictive analytical model. Langmuir 24:10107–10115

Dollet B, van Hoeve W, Raven JP, Marmottant P, Versluis M (2008) Role of the channel geometry on the bubble pinch-off in flow-focusing devices. Phys Rev Lett 100

Garstecki P, Hashimoto M, Shevkoplyas SS, Zasonska B, Szymborski T, Whitesides GM (2008) Formation of bubbles and droplets in parallel coupled flow-focusing geometries. Small 4:1795–1805

Kobayashi I, Nakajima M, Chun K, Kikuchi Y, Fujita H (2002) Silicon array of elongated through-holes for monodisperse emulsion droplets. AIChE J 48:1639–1644

Kobayashi I, Wada Y, Uemura K, Nakajima M (2008) Generation of uniform drops via through-hole arrays micromachined in stainless-steel plates. Microfluid Nanofluid 5:677–687

Kobayashi I, Wada Y, Uemura K, Nakajima M (2010) Microchannel emulsification for mass production of uniform fine droplets: integration of microchannel arrays on a chip. Microfluid Nanofluid 8:255–262

Kumacheva E, Li W, Greener J, Voicu D (2009) Multiple modular microfluidic (M(3)) reactors for the synthesis of polymer particles. Lab on a Chip 9:2715–2721

Li W, Young EWK, Seo M, Nie Z, Garstecki P, Simmons CA, Kumacheva E (2008) Simultaneous generation of droplets with different dimensions in parallel integrated microfluidic droplet generators. Soft Matter 4:258–262

McDonald JC, Whitesides GM (2002) Poly(dimethylsiloxane) as a material for fabricating microfluidic devices. Acc Chem Res 35:491–499

McDonald JC, Duffy DC, Anderson JR, Chiu DT, Wu HK, Schueller OJA, Whitesides GM (2000) Fabrication of microfluidic systems in poly(dimethylsiloxane). Electrophoresis 21:27–40

Miller E, Rotea M, Rothstein JP (2010) Microfluidic device incorporating closed loop feedback control for uniform and tunable production of micro-droplets and emulsions. Lab on a Chip 10:1293–1301

Mulligan MK, Rothstein JP (2011) The effect of confinement-induced shear on drop deformation and breakup in microfluidic extensional flows. Phys Fluids 23:022004

Nisisako T, Torii T (2008) Microfluidic large-scale integration on a chip for mass production of monodisperse droplets and particles. Lab on a Chip 8:287–293

Shu L, Eijkel JCT, van den Berg A (2007) Multiphase flow in microfluidic systems—control and applications of droplets and interfaces. Adv Coll Int Sci 133:35–49

van Dijke K, Veldhuis G, Schroen K, Boom R (2009) Parallelized edge-based droplet generation (EDGE) devices. Lab on a Chip 9:2824–2830

Vladisavljevic GT, Williams RA (2005) Recent developments in manufacturing emulsions and particulate products using membranes. Adv Coll Int Sci 113:1–20

Vladisavljevic GT, Kobayashi I, Nakajima M (2011) Effect of dispersed phase viscosity on maximum droplet generation frequency in microchannel emulsification using asymmetric straight-through channels. Microfluid Nanofluid 10:1199–1209

White FM (1991) Viscous fluid flow. McGraw-Hill, New York

Xu SQ, Nie ZH, Seo M, Lewis P, Kumacheva E, Stone HA, Garstecki P, Weibel DB, Gitlin I, Whitesides GM (2005) Generation of monodisperse particles by using microfluidics: control over size, shape, and composition. Angewandte Chemie-International Edition 44:724–728